Available online at www.sciencedirect.com
ScienceDirect
Surface Science 601 (2007) 5112–5115
SURFACE SCIENCE
www.elsevier.com/locate/susc

# Carbon nano dots scale by focused ion beam system for MIS diode nano devices

Ruslinda A. Rahim *, Hiroaki Kurahashi, Katsuhiro Uesugi, Hisashi Fukuda

*Faculty of Engineering, Department of Electrical and Electronic Engineering, Muroran Institute of Technology, 27-1 Mizumoto-cho, Muroran-shi, Hokkaido 050-8585, Japan*

Available online 4 May 2007

**Abstract**

Metal–insulator–semiconductor (MIS) structures with a nanocrystal carbon (nc-C) embedded in $SiO_2$ thin films were fabricated using a focused ion beam (FIB) system with a precursor of low-energy $Ga^+$ ion and carbon source. The crystallinity of nc-C was investigated by Raman spectroscopy and atomic force microscopy (AFM). Raman spectra indicate the evidence of crystallization of nc-C after annealed at 600 °C by the sharp peak at 1565 $cm^{-1}$ in graphite ($sp^2$), while no peak of diamond ($sp^3$) could be seen at 1333 $cm^{-1}$. The AFM images showed the nc-C dots controlled with diameter of 100 nm, 200 nm and 300 nm, respectively. The above results revealed that the nc-C dots had sufficiently stuck onto $SiO_2$ films. The hysterisis loop in the capacitance–voltage characteristics appeared in the MIS device with $SiO_2$/nc-C/$SiO_2$ structure in which voltage shift is 0.32 V for radical oxidation and 0.14 V for dry oxidation, respectively.


*Keywords:* Carbon; Nanocrystal; Memory device; Focused ion beam; Raman spectroscopy; Atomic force microscopy

## 1. Introduction

Metal–insulator–semiconductor field-effect transistor (MISFET) devices based on quantum dots and/or nanocrystal have recently attracted much interest both in new physical phenomena and potential applications toward next generation memory devices [1,2], where nanocrystal dots confined in the oxide layer between a control gate and a channel act as floating memory nodes. Nanocrystal (nc) in the MIS structure have memory characteristics in which charge storage is strongly influenced by several mechanism including quantum confinement effects, Coulomb charge effects, traps at interface and defect states [3–6,8,9]. It has been reported that electrons injected into nc might fall into a shallow traps near the conduction band edge [3,8]. The charge storage behavior in the nc including MIS structure was found to be related to the interface traps between $SiO_2$ and nc and the traps in nc or Si substrate except for quantum confinement. Because of the imperfection of interfaces between the nc and the Si substrate and/or interface of oxide surrounding nc, however, it is also expected that structural defects can be generated during the nc fabrication. Moreover, the hydrogen incorporated during the MIS structure fabrication will affect the interface trap states between nc and $SiO_2$. Therefore, it is necessary to study the traps in nc/$SiO_2$ interface and/or in the interface between substrate Si and $SiO_2$ film.

In this study, we will investigate the physical and chemical properties of nanocrystal carbon (nc-C) or amorphous carbon depending on the deposition techniques and film growth conditions. The experimental evidence for the effect of traps on the charge storage characteristic in the nc-C in $SiO_2$ films is demonstrated.

## 2. Experimental

The device fabrication was started with the (100)-oriented p-type silicon wafer (5–10 Ω cm), which were cut into 1.5 × 1.5 cm square chips as substrates. These chips were

* Corresponding author.
*E-mail address:* ruslinda_ar@yahoo.co.uk (R.A. Rahim).

0039-6028/$ - see front matter 
doi:10.1016/j.susc.2007.04.162

rinsed in de-ionized water and methyl alcohol, and processed by a standard RCA cleaning procedure. First, a $SiO_2$ film was grown on the Si in a dry oxygen ambient at 1000 °C for 20 min using a quartz furnace tube. Then, arrays of holes of 0.05 mm in diameter were created by photolithography process and 10 nm-thick tunnel $SiO_2$ film is formed in the holes by dry oxygen ambient at 1000 °C for 10 min. After oxidation, nc-C dots were deposited in regular intervals by using low-energy focused ion beam (FIB) technique in which phenanthrene ($CH_{14}H_{10}$) as a raw material is decomposed by focused $Ga^+$ ion with beam current of 49.3 pA at 30 kV. Then, 2 nm-thick control $SiO_2$ film was formed to cap the nc-C dots by two different methods using radical oxidation, i.e., atomic oxygen irradiations at 300 °C for 4 min and dry oxidation at 300 °C for 20 min. Direct observation of the nc-C in $SiO_2$ film was seen using scanning ion microscope (SIM) equipped with FIB system in the condition of a 30 kV as the acceleration energy. Raman spectra were obtained using a Raman spectrometer with a 514.5 nm line of an $Ar^+$ laser (100 mW) as the excitation source. Grain morphology was observed with atomic force microscopy (AFM) apparatus.

All electrical measurements were conducted on films of a MIS configuration. Several aluminium (Al) electrodes of 0.5 mm diameter were evaporated over the hole area of the films. After Al deposition, the sintering was performed at 350 °C for 10 min at $N_2$ ambient. Capacitance–voltage ($C$–$V$) measurement was carried out using a computer-controlled automatic electrical analyzer.

## 3. Results and discussion

Fig. 1a demonstrates an SIM cross sectional image by focused $Ga^+$ ion with beam current of 49.3 pA at 30 kV to confirm the thickness of 10 nm-thick $SiO_2$ film on Si film during dry oxidation process. Fig. 1b shows top view SIM image after carbon deposition by small beam current below 100 pA to minimize material removal during imaging [7]. The nc-C was confirmed to be a crystalline at the nanoscale region with a diameter of approximately 300 nm. The 2-dimensional density of nc-C is $3.4 \times 10^{12}$ $cm^{-2}$, the height and width of the nc-C dots were approximately 20 nm and 300 nm, respectively.

Fig. 2 shows the Raman spectra of nc-C dots produced by FIB under various conditions as-deposited at 25 °C (RT) and after annealed at 300 and 600 °C, respectively. The samples as-deposited and annealed at 300 °C indicate no specific peak, but several broad hump appear resulting in crystalline of diamond like amorphous carbon (a-DLC) [4]. The crystallization of a-DLC at 600 °C annealing is evidenced by the sharp peak at 1565 $cm^{-1}$ in graphite ($sp^2$), while no peak is seen at 1333 $cm^{-1}$ in diamond ($sp^3$) phase. The peak position hardly changes but it full width at half maximum (FWHM) increases as annealing temperature increases. For spherical crystals, the first-order Raman spectrum $I_c(\omega)$ is expressed by

$$I_c(\omega) = D \int_0^{q_{\max}} \frac{|C(O,q)|^2 \mathrm{d}q}{[\omega - \omega(q)]2 + (\Gamma_0/2)^2} \quad (1)$$

where $D$ is the intensity prefactor, $|C(O,q)|^2$ is the Fourier coefficient of the phonon confinement function, $\omega(q)$ is the phonon dispersion, and $\Gamma_0$ is the inverse lifetime of the phonon in bulk carbon [5]. We focus on the G-band position, which is related to the fraction of $sp^2$-bonded atomic sites. Increasing the power density in the a-DLC results in a higher G-band position, implying an even higher fraction of graphite ($sp^2$), this is presumably caused by the incorporation of H atoms into the lattice [4]. There is a small broad peak around 1378 $cm^{-1}$, which is attributed to a small

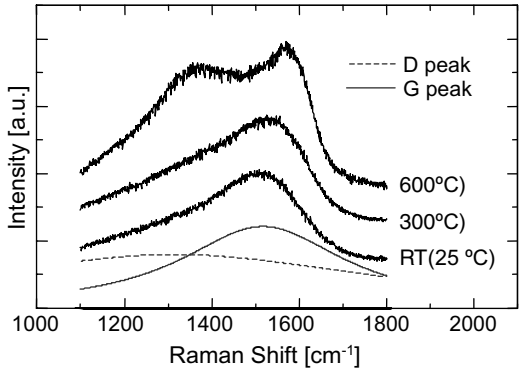


Fig. 2. Raman spectra for the nc-C in $SiO_2$ films as-deposited and after annealed.

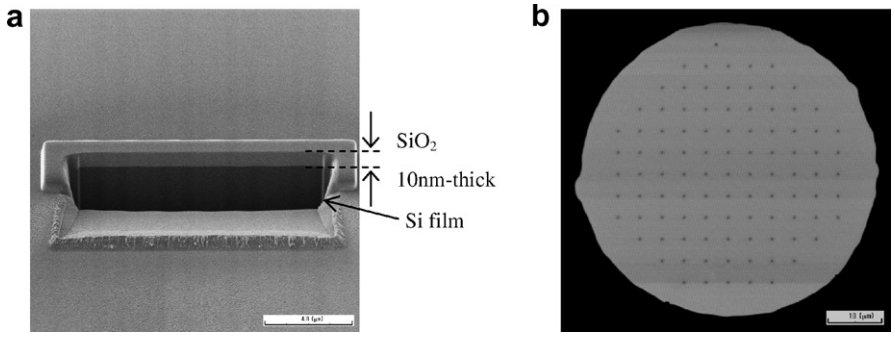


Fig. 1. SIM cross sectional images of $SiO_2$ film after dry oxidation process (a), array of nanocrystal carbon dots (b).

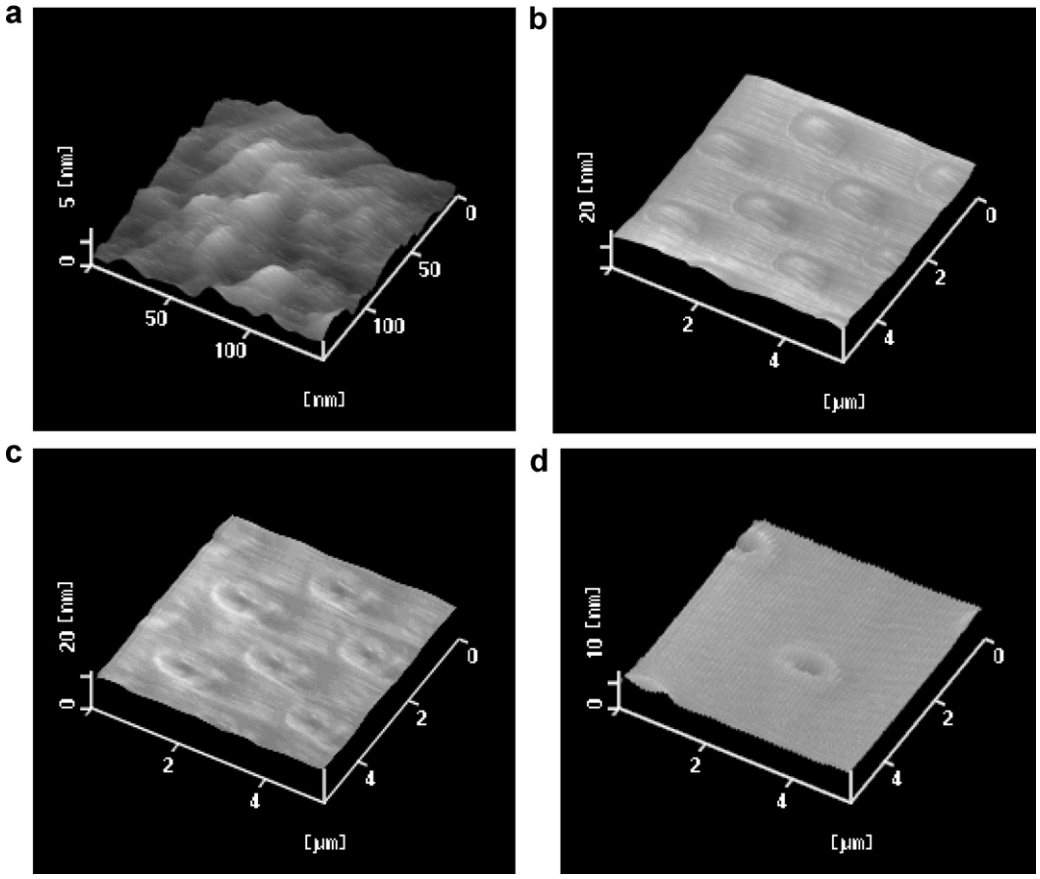


Fig. 3. AFM images of nc-C dots deposition; (a) morphology of a-DLC when annealing at above 400 °C in $N_2/H_2$ ambient, (b), (c) and (d) show the morphologies of nc-C dots at 100 nm, 200 nm and 300 nm, respectively. Average nc-C dots thicknesses are within 10–20 nm.

amount of a-C:H. This peak is not intense enough to fit to separate G- and D-bands. Thus, the facts shown in Fig. 2 reveal that the anneal process promotes the growth of nc-C dots.

Morphology of nc-C dots was investigated by AFM. In Fig. 3a, the morphology of a-DLC appears to be crystalline when the sample was carried out with annealed above 400 °C in $N_2/H_2$ ambient. This is considered that nitrogen and/or hydrogen are deliberately added to produced hydrogenated a-C:H and nitrogenated amorphous carbon a-C:N, respectively [4]. Fig. 3b, c and d show the nc-C dots with diameter 100 nm, 200 nm and 300 nm, respectively. It showed that the nc-C dots had sufficiently stick onto $SiO_2$ films, however, the dots seem to became like a hole, which tends to be wide at the top surface and tapers down to a point at the bottom of the hole. The formation of this 'V–shape' has been attributed to the deposition of sputtered material that occurs when deposit at high beam currents [7,10]. This is also considered the deposition time/refresh time/ion current is not optimum. The deposition

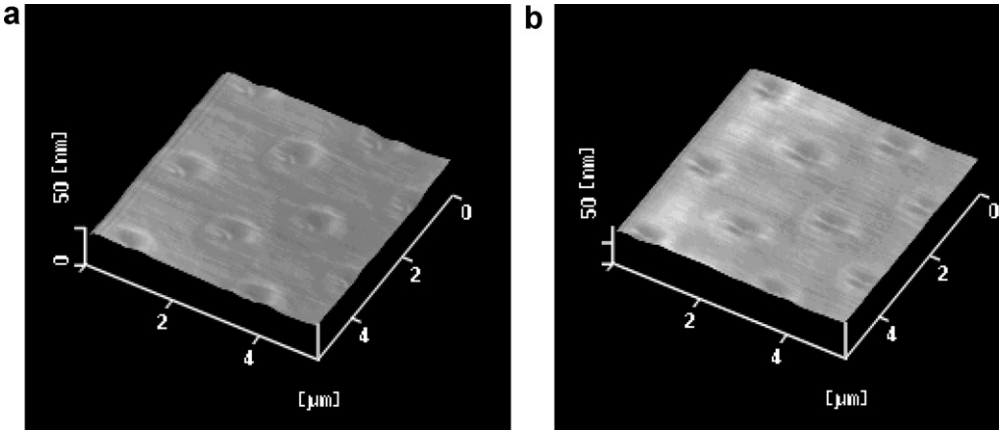


Fig. 4. AFM images of 200 nm after being capped with $SiO_2$ by two different methods; (a) radical oxidation, (b) dry oxidation.

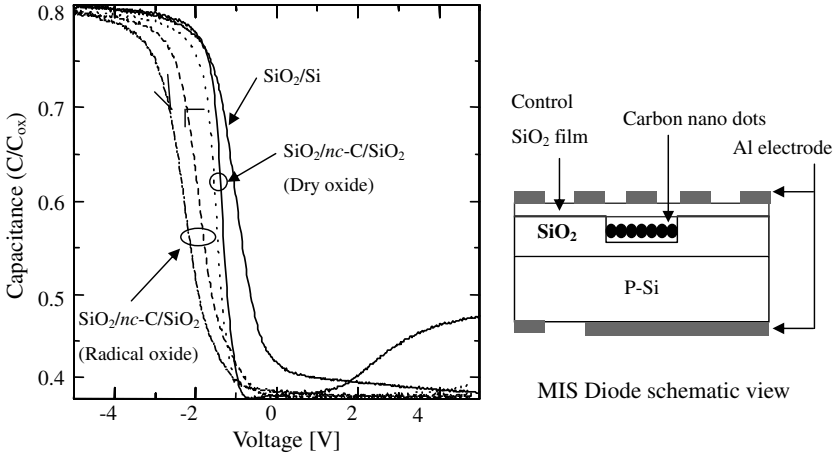


Fig. 5. (a) *C–V* hysterisis behavior for the MIS samples with nc-C and without nc-C, and (b) MIS Diode schematic view.

rate should be slowed. In addition, the deposited material properties will not be optimum due to incomplete decomposition resulting in incorporation of unwanted impurities [7,10].

In addition, the differences AFM images after being capped with $SiO_2$ by two different methods was shown in Fig. 4a and b, respectively. It showed that being capped by radical oxidation has maintained the shape crystalline of nc-C dots due the formation time is only 4 min. However, by dry oxidation method the crystalline of nc-C dots seem to be disappeared assuming it were diffusion by rapid temperature changed during the process.

Fig. 5a represents the capacitance–voltage (*C–V*) hysterisis behaviour of the MIS structure without nc-C and with nc-C, respectively. While Fig. 5b showed the schematic view of MIS Diode process. In the sample without nc-C, the hysterisis is not evident, and the flat band voltage ($V_{fb}$) is not obviously shifted. Thus, there is no charge storage. In contrast, the hysterisis loop of the sample with nc-C is clearly visible, especially for radical oxidation with the voltage difference is 0.32 V but in dry oxidation, although nc-C dots seems to be disappeared during capped $SiO_2$ but only a little hysterisis loop was seen with the voltage difference of 0.14 V. Generally, the memory effect can be explained by the injected charges stored in nc-C, the interface or the traps, in addition to dimension quantum confinement and Coulomb charge effects [11]. If a nc-C based MIS structure exists, the fixed charge in $SiO_2$, $V_{fb}$ will be negatively shifted, and therefore it is necessary to consider the deep levels in nc-C in addition to the interface traps between $SiO_2$ and Si. In the sample with nc-C, a little shifts of $V_{fb}$ are seen. One apparent reason is the captured electrons or holes into nc-C. However, compared with $SiO_2$, H incorporated in nc-C during growth and it can play an important part of the memory effects in a MIS structure with nc-C [12]. Through *C–V*, we suggest that the traps related to the hydrogen and the interface between substrate Si and $SiO_2$ including quantum confinement and Coulomb charge effect influenced the memory behavior of a MIS structure with nc-C.

## 4. Conclusions

In summary, we have fabricated successfully a carbon nanocrystal embedded in $SiO_2$ film by using focused ion beam technique. The crystallization of carbon at least above 300 °C annealing was confirmed by Raman spectra and atomic force microscopy. The capacitance–voltage showed hysterisis behavior due to charge storage in a MIS structure with nc-C in which the quantum confinement and Coulomb charge effects are dominant in the deep levels related to the hydrogen and interface between Si substrate and $SiO_2$ film.

## Acknowledgement

This work was supported by a Grant-in-Aid for Scientific Research from the Ministry of Education, Science, Sports and Culture (No.17510107).

## References

[1] S. Tiwari, F. Rana, H. Hanafi, A. Harstein, E. Crabbè, K. Chan, Appl. Phys. Lett. 68 (1996) 1377.
[2] A. Dutta, Y. Hayafune, S. Oda, Jpn. J. Appl. Phys. 1 39 (2000) 855.
[3] S. Tiwari, F. Rana, K. Chan, L. Shi, H. Hanafi, Appl. Phys. Lett. 69 (1996) 1232.
[4] Bharat Bhushan (Ed.), Handbook of Nano–Technology, Springer, 2004, p. 800.
[5] H. Fukuda, S. Sakuma, T. Yamada, S. Nomura, M. Nishio, T. Higuchi, S. Ohshima, J. Appl. Phys. 90 (2001) 3524.
[6] G. Iannacone, P. Coli, Appl. Phys. Lett. 78 (2001) 2046.
[7] L.A. Giannuzzi, F.A. Stevie (Eds.), Introduction to Focused Ion Beams: Instrumentation, Theory, Techniques and Practice, Springer, 2005, p. 13.
[8] Y. Shi, K. Saito, H. Ishikuro, T. Hiramoto, J. Appl. Phys. 84 (1998) 2358.
[9] N. Takahashi, H. Ishikuro, T. Hiramoto, Appl. Phys. Lett. 76 (2000) 209.
[10] J. Orloff, M. Utlaut, L. Swanson (Eds.), High Resolution Focused Ion Beams: FIB and Its Application, Kluwer Academic, 2003, p. 21.
[11] Y.H. Kwon, C.J. Park, W.C. Lee, D.J. Fu, Y. Shon, T.W. Kang, C.Y. Hong, H.Y. Cho, K.L. Wang, Appl. Phys. Lett. 80 (2002) 14.
[12] S.J. Pearton, T.W. Corbett, M. Stavola (Eds.), Hydrogen in Crystalline Semiconductor, Springer, Berlin, 1992, p. 4.